recycling

MDPI

Article

Resource Recovery from Abandoned Mine Drainage Galleries via Ion Exchange: A Case Study from Freiberg Mining Area, Germany

Janith Abeywickrama [1,*], Katayoun Karimi [1], Marlies Grimmer [2], Nils Hoth [1] and Carsten Drebenstedt [1]

[1] TU Bergakademie Freiberg, Institute of Mining, Gustav-Zeuner-Straße 1a, 09599 Freiberg, Germany; katayoun.karimi-razakani@mabb.tu-freiberg.de (K.K.); nils.hoth@tu-freiberg.de (N.H.); carsten.drebenstedt@mabb.tu-freiberg.de (C.D.)
[2] Wismut GmbH, Jagdschänkenstraße 29, 09117 Chemnitz, Germany; m.grimmer@wismut.de
* Correspondence: janith.abeywickrama@mabb.tu-freiberg.de

Abstract: The discharge of metal-loaded mining-influenced waters can significantly pollute downstream water bodies for many kilometers. Addressing this issue at the earliest discharge point is crucial to prevent further contamination of the natural environment. Additionally, recovering metals from these discharges and other sources of contamination can reduce the environmental impacts of mining and support the circular economy by providing secondary raw materials. This study focused on optimizing zinc recovery from mining-influenced water in the Freiberg mining region in Germany, where significant loads of zinc are released into the Elbe River. By employing pretreatment techniques, conducting 100 mL scale ion-exchange column experiments, and refining the regeneration process, we aimed to identify optimal conditions for efficient zinc removal and recovery. Initial tests showed that aminophosphonic functionalized TP 260 resin had a high affinity for aluminum, occupying 93% of the resin's capacity, while zinc capacity was limited to 0.2 eq/L. To improve zinc recovery, selective precipitation of aluminum at pH 6.0 was introduced as a pretreatment step. This significantly increased the zinc loading capacity of the resin to 1 eq/L. Under optimal conditions, a concentrated zinc solution of 18.5 g/L was obtained with 100% recovery. Sulfuric acid proved more effective than hydrochloric acid in eluting zinc from the resin. Further analysis using SEM-EDX revealed residual acid on the resin, indicating a need for additional study on long-term resin performance and capacity variation. The research also highlighted the environmental impact of the Freiberg mining area, where three drainage galleries currently contribute nearly 85 tons of zinc annually to the Elbe River. This study underscores the feasibility of efficient zinc recovery from these point sources of pollution using advanced ion-exchange processes, contributing to circular economy efforts and environmental conservation.

Keywords: acid mine drainage; zinc; ion-exchange recovery; separation

check for updates

Citation: Abeywickrama, J.; Karimi, K.; Grimmer, M.; Hoth, N.; Drebenstedt, C. Resource Recovery from Abandoned Mine Drainage Galleries via Ion Exchange: A Case Study from Freiberg Mining Area, Germany. *Recycling* **2024**, *9*, 105. https://doi.org/10.3390/recycling9060105

Academic Editor: Akira Otsuki

Received: 23 July 2024
Revised: 18 October 2024
Accepted: 30 October 2024
Published: 2 November 2024

1. Introduction

As industries continue to expand and technological advancements drive further demand, the sustainability of metal resources becomes increasingly uncertain [1,2]. This underscores the importance of exploring alternative sources, enhancing recycling efforts, and developing more efficient extraction techniques to mitigate the potential impact of metal scarcity on various sectors of the economy [3,4].

Conversely, industries like mining produce various waste types containing metal pollutants, posing environmental risks due to their harmful impact on public health and natural habitats [5–8]. Therefore, recovering metals from secondary sources such as mine waste and mining-influenced water serves two vital purposes: ensuring environmental sustainability and meeting the global economy's raw material demands. Water impacted by mining raises environmental concerns due to its lower pH levels and elevated concentrations of dissolved and particulate forms of metals [9–11]. Numerous mining operations generate substantial volumes of mining-affected water, which may continue to be discharged into the environment for many decades following mine closure [12–14]. However, mining-influenced waters also serve as a potential secondary source of metals.

The Erzgebirge region in Saxony, Germany, has a rich history of mining dating back centuries. The area is well-known for its various ore deposits, including silver, tin, zinc, and other metals [15,16]. The mining operations in the region have been influential in shaping both the economy and cultural legacy of the area. However, many mines have closed over time due to economic and environmental factors [17]. The Reiche Zeche, a former silver mine in the Freiberg district, Saxony, Germany, is notable for its extensive network of mine water drainage galleries that act as point sources of mining-influenced water discharge to the surrounding river systems [18,19].

According to the literature, the deepest discharge gallery, the Rothschönberger Stollen (RSS), dewaters the Freiberg mine waters 18 Km north of Freiberg into the Triebisch River [18]. The "Königliche Verträgliche Gesellschaft Stollen" (VGS) and the "Hauptstolln Umbruch" (HSU) discharge some parts of the Mine drainage into the Freiberger Mulde river [20,21]. Noteworthy, the mine water discharge galleries in the Freiberg area play a significant role, contributing 37% of the zinc contamination found in the Elbe River [22]. Recent studies have also indicated elevated zinc concentrations of up to 20 mg/L and lower pH levels in waters discharged from specific old galleries [20]. These galleries, often referred to as dewatering galleries, are structures designed to remove water from the mine to prevent flooding and facilitate mining operations. Zinc is a vital endangered metal, a pivotal element across various industrial sectors, and essential for sustaining life on Earth. As per the global annual mining statistics per capita, approximately 30% of this output originates from recycling efforts [23,24]. Hence, the mining-influenced water in the Freiberg area presents promising opportunities to recover zinc from these dewatering galleries.

The need for sustainable approaches to treating mining-influenced water highlights the importance of coupling metal removal with resource recovery. While metal precipitation has been extensively studied as a wastewater treatment method, efficient metal recovery remains a significant challenge [25]. Several studies indicate that hydrometallurgical processes also extract metals from mine wastes. For instance, sulfuric acid leaching combined with solvent extraction has been shown to achieve high recovery rates, with over 70% of zinc recovered from mine wastes and mining-influenced water [26,27]. However, this method requires large quantities of acid, which increases costs and poses environmental risks due to potential acid runoff. Additionally, the process demands significant space for plant setup, making it less viable for small-scale operations. Bioleaching has also demonstrated promising results, with recovery rates of up to 95% for copper and 80% for zinc from mine wastes [28]. However, the bioleaching process is slow, as microbial action takes an extended time to break down the ores, which can delay metal recovery. In the last decade, an increasing number of researchers have shifted their focus towards investigating alternative methods like sorption [29,30], membrane filtration [31,32], and ion exchange [33,34] for extracting metals from water affected by mining activities. These emerging methods offer promising avenues to tackle environmental challenges and meet economic objectives simultaneously.

Among these alternative methods, ion exchange (IX) stands out for its numerous advantages. These include its high selectivity for specific ions, improved recovery rates, reduced sludge production, rapid kinetics, and ability to meet stringent discharge limitations [33,35]. Many researchers favor synthetic resins due to their superior efficiency compared to natural materials [35–40]. Nonetheless, ion exchange remains widely acknowledged as a highly efficient method for eliminating and reclaiming various metal ions such as copper [41,42], cobalt [43,44], nickel [35,45], zinc [33,46], including rare earth elements [47,48]. In a study by Sole [36], the focus was on eliminating zinc using ion exchange. Employing the Lanxess aminophosphonic acid resin, TP 260, successfully reduced zinc levels from 30 mg/L to below 1 mg/L. Abeywickrama et al. [33] utilized a resin containing aminophosphonic acid to extract zinc from mine water in the Erzgebirge area of Germany. Subsequently, through the de-loading process involving sulfuric acid, they achieved a zinc concentrate yield of 12 g/L with a recovery rate exceeding 85%. However, metal concentrates within the 30–40 g/L range are essential for efficiently employing the electrowinning technique to recover specific metals [36,37]. Therefore, if achieving these concentrations proves economically unfeasible, an alternative strategy involves utilizing the metal-enriched solutions as an additional resource for metal refinery operations.

This study concentrates on developing a technique for selective zinc recovery from the mining-influenced water in the Freiberg area. Specifically, our focus lies on (i) analyzing the water quality parameters in various mine drainage galleries and recipient streams, (ii) assessing the zinc loading capacity of chelating ion-exchange resin featuring an aminophosphonic acid functional group, (iii) optimizing metal recovery through water pretreatment, and (iv) comparing zinc recovery using various regenerant solutions. The successful application of this technique can significantly reduce the discharge of mining-influenced metal loads into natural streams while also producing a valuable secondary product, such as a metal concentrate, that can contribute to a circular economy.

2. Results and Discussion

2.1. Mine Water Chemistry

The relationship of the milieu parameters of the discharged gallery waters is presented in Figure 1a,b. Different galleries can be easily differentiated based on milieu parameters except for a few data points. All mine waters are generally oxidized and show a higher redox potential compared to river water samples in that they were discharged. The discharge water of the VGS gallery shows a characteristic low pH (4.5–6.0) and higher conductivity values (0.8–1.4 mS/cm) at a similar temperature and Eh ranges compared to other mine water discharge galleries. RSS discharge water always had a 2–3 °C higher temperature than the other galleries. VGS and HSU galleries had 5–6 °C higher temperature and redox values than the Mulde river (FM) where they were discharged.

Table 1 summarizes the hydrochemical parameters of all three discharge galleries. Generally, mine waters are rich in calcium and sulfate while low in sodium and carbonate. Noteworthy, VGS shows very low bicarbonate and is compatible with lower pH. However, HSU and RSS show good buffering against the low pH (also shown in Figure 1a). However, the river water samples (in Mulde and Triebisch (TRI)) acquired from the upstream of the discharge galleries show relatively lower sulfate and increased bicarbonates.

In the present study, the concentration of Fe and Al in the "total" fraction was found to be much higher than the "dissolved" fraction for all VGS and HSU water galleries (Figure 1c). Water samples from RSS and Triebisch River show a minimum value (close to zero) of dissolved and particulate metal ions. On the other hand, HSU and Mulde river samples show an increment of particulate Fe and Al in the water samples (0.1–0.5 meq/L).

In contrast, VGS samples show a wide range and increased amount of particulates of iron and aluminum in the water (0.5–2.6 meq/L). It should be noted that the highest particulate values (shown with a blue circle; Figure 1c) in the VGS were always observed after the heavy rain events. All mine water discharge clearly indicates an elevated level of sulfate concentration compared to receiving river systems (Figure 1d). VGS indicated the highest and wide range of sulfate (6–11 meq/L) and chloride (2.5–5.5 meq/L) values, whereas RSS and HSU show a similar range of sulfate values (4–6 meq/L). The VGS waters show a wide range of sulfate concentrations (4.79–10.42 meq/L) compared to RSS (4.38–6.25 meq/L) and HSU (1.67–2.48 meq/L). The discharge of the RSS was characterized by low chloride concentrations (1.72–2.23 meq/L) compared to VGS and HSU waters (Figure 1d). Zinc is considered one of the most important contaminant discharges from mine water galleries in the Erzgebirge area. At all times, all three mine water galleries discharge zinc at concentrations higher than the German threshold limit of 0.015 meq/L (equivalent to 0.5 mg/L). The discharge from the VGS gallery shows significantly higher zinc concentrations (0.245–0.673 meq/L) compared to the HSU (0.061–0.306 meq/L) and RSS (0.077–0.138 meq/L).

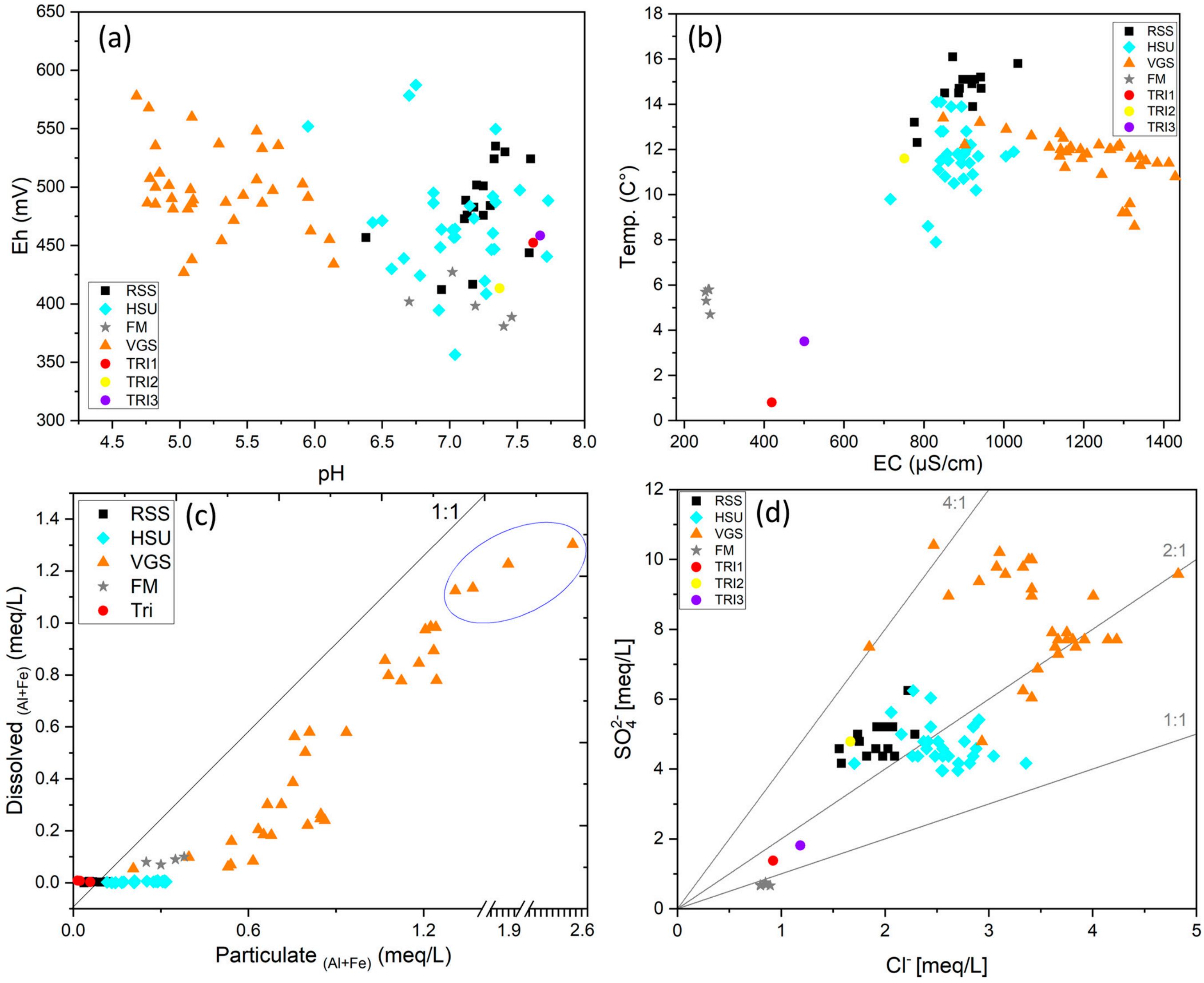

Figure 1. (**a**) Pourbaix (Eh-pH) diagram; (**b**) Temperature versus electrical conductivity diagram of the Erzgebirge mine waters; (**c**) Ratio of Particulate to dissolve Al + Fe; (**d**) The relationship between Chloride and Sulfate.

Table 1. Summary of main hydrochemical parameters for mine water galleries in the Freiberg area (from this study).

Gallery Name	HSU Water (n = 23)				VGS Water (n = 26)				RSS Water (n = 12)			
Parameter	**Min**	**Max**	**Mean**	**Stdv**	**Min**	**Max**	**Mean**	**Stdv**	**Min**	**Max**	**Mean**	**Stdv**
Flowrate (L/s)	37.0	134	69.2	30.4	25.3	48.0	33.4	6.0	262	520	466	93.3
T (°C)	10.5	14.1	12.2	1.0	10.8	13.4	11.9	0.7	14.5	16.1	15.1	0.5
EC (µs/cm)	832	1005	881	40.8	848	1429	1217	149.7	852	1035	915	48.8
pH	6.5	7.7	7.2	0.3	4.7	6	5.3	0.5	7.1	7.6	7.3	0.1
Eh (mV)	409	550	466	30.5	427	578	488	37.2	473	530	496	21.2
Na (mg/L)	23.1	49.0	30.1	5.6	20.2	48.4	33.3	7.8	27.6	40.6	34.2	3.9
K (mg/L)	3.4	10.8	5.3	1.6	2.7	8.4	5.2	1.1	4.4	5.8	4.9	0.5
Mg (mg/L)	20.9	29.8	24.7	2.4	23.0	44.4	37.8	4.9	20.5	26.2	23.6	2.0

Table 1. *Cont.*

Gallery Name	**HSU Water (n = 23)**				**VGS Water (n = 26)**				**RSS Water (n = 12)**			
Parameter	**Min**	**Max**	**Mean**	**Stdv**	**Min**	**Max**	**Mean**	**Stdv**	**Min**	**Max**	**Mean**	**Stdv**
Ca (mg/L)	47.0	117	78.2	17.6	46.0	183	118	30.0	86.4	129	102	12.3
Al (mg/L)	0.2	2.6	0.9	0.6	1.7	18.5	7.7	3.9	0.1	0.3	0.2	0.0
Fe (mg/L)	1.8	10.1	3.4	1.9	0.3	11.1	1.8	2.3	0.5	1.5	0.8	0.3
Mn (mg/L)	1.9	5.6	3.6	0.8	3.9	11.2	7.8	1.7	0.4	0.8	0.7	0.1
Si (mg/L)	8.3	10.6	9.8	0.6	6.6	10.4	8.9	1.0	8.7	10.1	9.3	0.4
Zn(mg/L)	1.5	10.3	4.6	2.3	8.0	21.5	16.0	3.7	2.5	4.2	3.6	0.5
Cl^- (mg/L)	190	300	222	29.2	87.5	171	122	18.8	61.6	78.8	70.1	4.7
$SO_4{}^{2-}$ (mg/L)	80.3	119	94.8	9.5	230	500	406	73.7	210	300	237	27.2
TIC (mg/L)	0.81	1.54	1.16	0.3	1.21	3.51	2.86	1.1	1.17	3.55	2.51	1.0
TN (mg/L)	1.61	3.59	2.45	0.9	1.53	3.51	2.86	1.5	2.52	3.79	2.14	0.8

2.2. Zinc-Adsorption Isotherms

The equilibrium statuses during batch adsorption studies can be generally explained by isotherm modeling, which is characterized by parameters reflecting the surface properties and attraction of the adsorbent. This study employed the Langmuir and Freundlich isotherms to establish a relationship between the amount of zinc ions adsorbed by TP 260 resin and their equilibrium concentrations in both synthetic and VGS mine water.

The Langmuir isotherm assumes a single monolayer formed through the reaction, with specific binding sites, immobile adsorbates, and no adsorbate-adsorbent interaction. When comparing the two models, it represents high sorption, while the Freundlich isotherm reflects an infinitely layered scenario [49]. The specific form of the Langmuir equation is presented in Figure S1. Correlation coefficients for the Langmuir and Freundlich models were 0.99 and 0.65 for synthetic water and 0.97 and 0.78 for VGS mine water (20 mg/L), respectively (Table 2). These results suggest that the Langmuir isotherm effectively describes zinc adsorption onto TP 260 resin, indicating a monolayer adsorption process on the uniformly distributed active sites of the TP 260 resin surface.

Table 2. Adsorption isotherm parameters for zinc removal with synthetic and VGS mine waters.

	Langmuir				**Freundlich**			
	Zn	**q_m**	**K_m**	**R^2**	**Zn**	**K_f**	**N**	**R^2**
	(mg/L)	**(mg/g)**	**(L/mg)**		**(mg/L)**	**(mg/g)**		
Synthetic water	10	37.45	133	0.99	10	1.21	136.99	0.65
	20	60.24	11.06	0.99	20	1.15	156.25	0.34
VGS water	10	20	4	0.98	10	1.51	10.7	0.73
	20	24	1	0.97	20	1.13	25.06	0.78

2.3. Pretreatment of the Mine Water

Increasing the pH to 6 leads to forming an aluminum hydroxide precipitate, which removes about 92% of the dissolved aluminum from the water (Figure S2). This precipitation of aluminum reaches 100% as the pH is raised to 7. However, at pH 8, aluminum removal slightly decreases due to the redissolution of aluminum hydroxide. Zinc precipitation begins around pH 5.5 and reaches 100% at a pH of 8. Based on these findings, pH 6 was determined to be the optimal level for pretreatment as it removes most of the aluminum in the water with minimal zinc removal (approximately 15%). However, scaling up this process to an industrial level may result in the generation of sludge that requires further treatment. A previous study by Abeywickrama et al. [45] demonstrated that aluminum could be selectively adsorbed onto TP 209 resin via ion exchange in a batch reaction with a slag-leaching residue solution. Building on these findings, further studies need to be conducted to focus on the selective adsorption of aluminum onto the resin. The goal is to produce a concentrated aluminum product that can be reintroduced into the circular economy, enhancing sustainability and resource efficiency.

2.4. Recovery of the Zinc via Ion Exchange

The results of the ion-exchange experiment conducted for the recovery of Zn from mine water discharge in the VGS gallery are summarized in Figure 2. During the first phase, two columns filled with fresh TP 260 resins were loaded with untreated mine water from the VGS gallery. When untreated mine water was introduced into the ion-exchange columns (columns V1 and V2), the breakthroughs of both Al and Zn occurred around 500-bed volumes (Figure 2a). Notably, Al exhibited a gradual breakthrough curve showing a higher affinity for the TP 260 resin. In contrast, Zn showed a steep curve, reaching exhaustion at approximately 750 BVs and desorbing until the end of the loading experiment. This desorption is likely due to the higher affinity of the resin for aluminum ions, which leads to the displacement of zinc ions as the resin becomes saturated with aluminum. Several other authors also exhibited a higher selectivity of the Al towards the aminomethylphosphonic functional group [50,51].

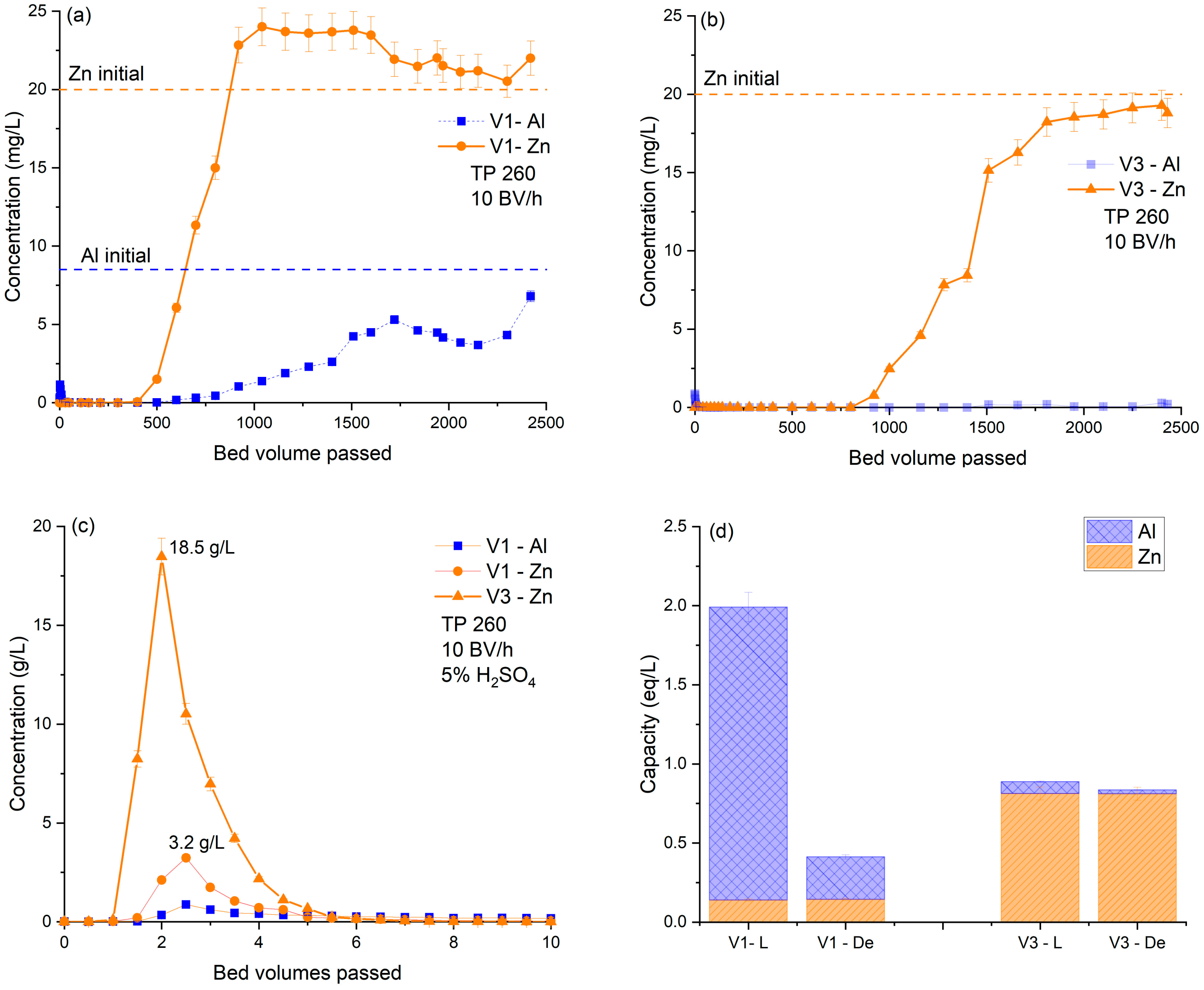

Figure 2. (**a**) Breakthrough curves of untreated mine water (Zn and Al) loaded into IX column with TP 260 resin; (**b**) breakthrough curves of pretreated mine water (after Al precipitation); (**c**) De-loading curves of Zn and Al in untreated (column A) and pretreated (column B) mine waters; (**d**) Mass balance of column A and B (L—loading, De—De-loading).

Consequently, additional measures were implemented to eliminate Al as a pretreatment, as described in the preceding subchapter. Subsequently, aluminum-free mine water (pretreated) was pumped into two additional columns. Column V3 was filled with fresh TP 260 resin, while column V4 utilized the second cycle of the V2 column after the de-loading with sulfuric acid (employed in the previous experiment with untreated water).

In column V3 (fresh resin), the breakthrough points of Zn extended to 1000 BVs, with exhaustion reached at nearly 2500 BVs (Figure 2b). In the absence of Al, the resin's zinc retention capacity increased to 1 eq/L, compared to 0.14 eq/L when Al was present. During the de-loading of column V3, a Zn concentrate of 19 g/L (Figure 2c) was produced without any co-elution of the Al. In column V4, where the resin from the previous cycle was employed, Zn breakthrough occurred prematurely, approximately after 80-bed volumes. This can be attributed to the partial removal of Al during the de-loading process of the previous cycle. Consequently, the resin in column V4 was predominantly saturated with Al loaded during the previous loading cycle.

Mass balance results of the regeneration experiments of columns V1 and V2 indicated that nearly 14% of Al was able to de-load during the regeneration process (Figure 2d). Remarkably, in all cases, Zn recovery approached 100% (Table 3). These findings highlight the effectiveness of the ion-exchange process in selectively recovering zinc from mine water discharge, notably when aluminum is excluded as a pretreatment.

Table 3. Mass Balance for zinc and aluminum in columns V1, V2, V3, and V4 (in meq).

Column	**Loading**	**De-Loading**	**Remained**
Zinc			
V1	14.6 ± 0.7	14.5 ± 0.7	0.1 ± 0.005
V2	16.9 ± 0.8	16.6 ± 0.8	0.3 ± 0.015
Aluminum			
V1	185 ± 9.2	26.8 ± 1.3	158 ± 7.9
V2	211 ± 10.5	30.7 ± 1.5	181 ± 9.1
Zinc			
V3	81.3 ± 4.1	81.2 ± 4.1	0.04 ± 0.002
V4	23.9 ± 1.2	28.3 ± 1.4	-
Aluminum			
V3	7.30 ± 0.4	2.3 ± 0.1	4.97 ± 0.2
V4	5.04 ± 0.3	49.6 * ± 2.4	-

* Note–excess de-loading of Zn and Al in column V4 resulted from the incomplete de-loading of ions in previous cycles (V1 and V2).

2.5. Effect of Regenerant on Metal Recovery

Figure 3a,b present the de-loading profiles of Zn and Al, respectively, for columns V1 and V2. Both columns were subjected to loading with untreated mine water. The Zn de-loading process commenced at 0.5-bed volume in both columns and peaked and 3 bed volumes. Most of the zinc de-loading was completed by 5-bed volume. Notably, the column treated with 5% HCl exhibited a peak zinc concentration of 1.9 g/L, whereas the column treated with 5% H_2SO_4 acid showed a higher peak zinc concentration of 3.5 g/L.

Similarly, the Al elution also initiated at 0.5-bed volume and persisted until the cycle's completion at 10-bed volumes without reaching the baseline. The Al concentrations surged to 0.75 and 0.88 g/L for columns V1 and V2, respectively. Table 3 shows the mass balance of Zn and Al for all four column experiments. It is evident from Table 3 that at the end of the loading process, the resin capacity was predominantly occupied by Al ions (around 93%) in the first two columns (V1 and V2), with only 14 and 16 meq (around 7% of its operational capacity) of zinc being adsorbed. After the de-loading process, almost all the zinc ions were recovered, and most of the aluminum ions stayed within the resin. Significant enhancement in de-loading efficacy was noted in pretreated columns V3 and V4 (refer to Figure 3c,d) upon their treatment with 5% H_2SO_4 acid.

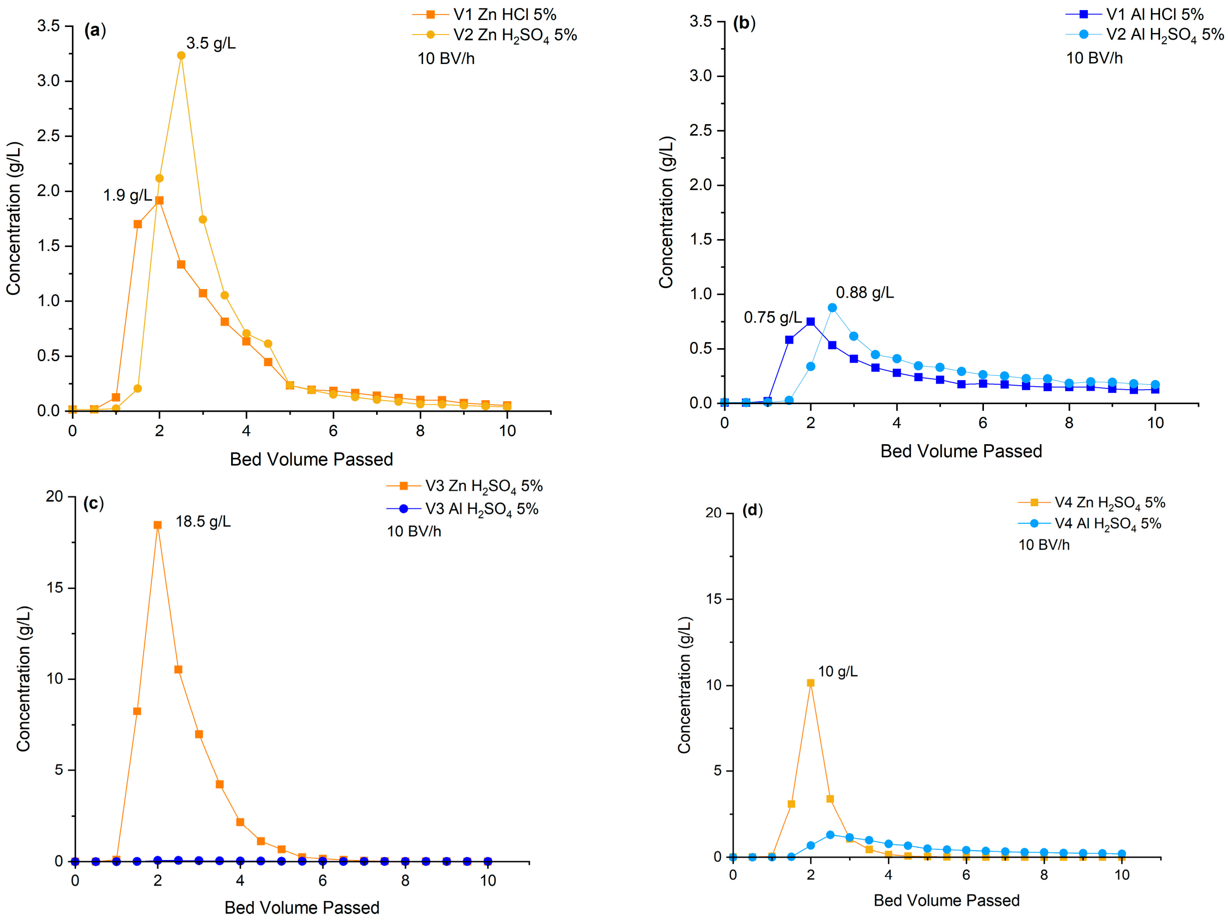

Figure 3. De-loading curves for (**a**) zinc and (**b**) aluminum in columns V1 and V2; column V1 was regenerated with 5% HCl, and column V2 was regenerated with 5% H_2SO_4 acid; (**c**) de-loading curves for column V3, and (**d**) column V4.

In column V3, featuring fresh resin, a peak concentration of 18.5 g/L was attained. Conversely, in column V4, utilizing previously used resin, a peak concentration of 10 g/L was observed, albeit accompanied by some aluminum co-elution from the preceding loading cycle. The results suggest that aluminum adsorption onto the resin TP 260 may permanently reduce the operational capacity of the resin. Moreover, aluminum cannot be readily deloaded from resin TP 260 via 5% H_2SO_4. Further investigation into the physical status of the resin using SEM-EDX was conducted later to understand aluminum adsorption onto the TP 260 resins.

Mass balance results also indicated that only 14% of the aluminum was able to de-load during the de-loading process. Remarkably, in all cases, Zn recovery approached 100%. From the overall mass balance perspective, it is apparent that the zinc capacity of the resin can be increased up to 1 eq/L when aluminum is absent in the system, compared to the mere 0.14 eq/L capacity observed in its presence. According to the resin manufacturer, the maximum capacity of the resin is stated to be 2.4 eq/L [52]. However, the highest operational zinc capacity documented in the literature is 1.8 eq/L, obtained under specific conditions of 30 mg/L zinc concentration and a water pH of 4.5 [53]. This indicates that further optimization of zinc capacity could be achieved through pH manipulation of the aqueous phase. Future research should focus on enhancing zinc recovery while considering the cost-benefit implications of pH adjustments and zinc capacity improvements. However, these findings highlight the effectiveness of the ion-exchange process in selectively recovering zinc from mine water discharge, particularly when aluminum is excluded as a pretreatment.

2.6. Characterization of the Physical Status of the Used Resins

Figure 4 illustrates the outcomes of an EDX analysis conducted on the initial state of the ion-exchange resin (TP 260) utilized in this investigation, outlining the elemental composition alongside respective measurements. Accompanying the measured values are normalized mass percentages and atom percentages, offering insights into the relative prevalence of each element. Furthermore, the table incorporates absolute error percentages, reflecting the degree of uncertainty linked with the measurements. Accordingly, carbon, oxygen, and phosphorus emerge as the predominant elements, comprising 49.61%, 30.75%, and 8.48% of the mass on the resin surface. Notably, the elevated sodium content observed in the resin (11.06%) arises from sodium ions on the resin, serving as counter ions to neutralize the anionic functional group (amino methyl phosphorus group).

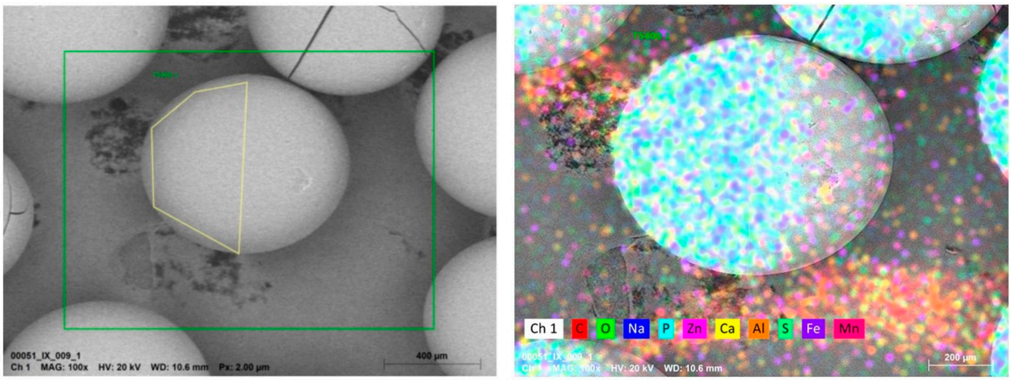

T5400 1

Element	At.No.	Netto	Mass [%]	Mass Norm. [%]	Atom [%]	abs. error [%] (1 sigma)	rel. error [%] (1 sigma)
C	6	1664	54.81	49.61	60.65	3.27	5.97
O	8	1153	33.97	30.75	28.22	2.1	6.18
Na	11	2608	12.22	11.06	7.06	1.56	12.74
Al	13	13	0.04	0.04	0.02	0.04	93.33
P	15	3187	9.37	8.48	4.02	0.88	9.38
S	16	16	0.06	0.06	0.03	0.04	69.37
Ca	20	0	0.00	0.00	0.00	0.00	0.91
Mn	25	0	0.00	0.00	0.00	0.00	0.65
Fe	26	0	0.00	0.00	0.00	0.00	0.64
Zn	30	0	0.00	0.00	0.00	0.00	0.69
		Sum	110.47	100.00	100.00		

Map

Element	At.No.	Netto	Mass [%]	Mass Norm. [%]	Atom [%]	abs. error [%] (1 sigma)	rel. error [%] (1 sigma)
C	6	8856	66.02	57.00	66.77	3.56	5.40
O	8	3744	34.73	29.98	26.37	1.95	5.60
Na	11	6072	6.97	6.02	3.68	0.61	8.74
Al	13	141	0.16	0.14	0.07	0.03	19.82
P	15	8040	7.93	6.84	3.11	0.5	6.35
S	16	0	0.00	0.00	0.00	0.00	1.57
Ca	20	14	0.02	0.02	0.01	0.02	124.79
Mn	25	0	0.00	0.00	0.00	0.00	0.65
Fe	26	0	0.00	0.00	0.00	0.00	0.64
Zn	30	0	0.00	0.00	0.00	0.00	0.69
		Sum	115.82	100.00	100.00		

Figure 4. SEM-EDX observation of the Initial stage of the TP 260 resin.

Figure 5 shows the elemental composition of deloaded TP 260 resins with 5% hydrochloric acid (Figure 5a) and 5% sulfuric acid (Figure 5b). Compared to the initial stage of the resin shown in Figure 4, the deloaded resin showed the absence of sodium ions from the resin matrix, suggesting the complete occupation of the resin capacity by other ions. However, the resin also indicates the availability of a considerable amount of aluminum after the de-loading process. This suggests that neither acid was able to completely remove aluminum during the de-loading process. This confirms the mass balance results explained in Table 3 and suggests the importance of the pre-removal of aluminum before the ion-exchange process.

The resin deloaded with hydrochloric acid exhibited a minor presence of zinc (0.1%), whereas the resin treated with sulfuric acid showed no detectable zinc on the resin surface (Figure 5). Mass balance calculations of the zinc recovery also suggest that sulfuric acid is more effective in removing zinc than hydrochloric acid. However, the significant difference in zinc content was not apparent through EDX measurements. Furthermore, the resin deloaded with HCl displayed a chloride mass of 5.6%, while the resin regenerated with sulfuric acid showed a sulfur content of 6.3% on the resin surface (Figure 5).

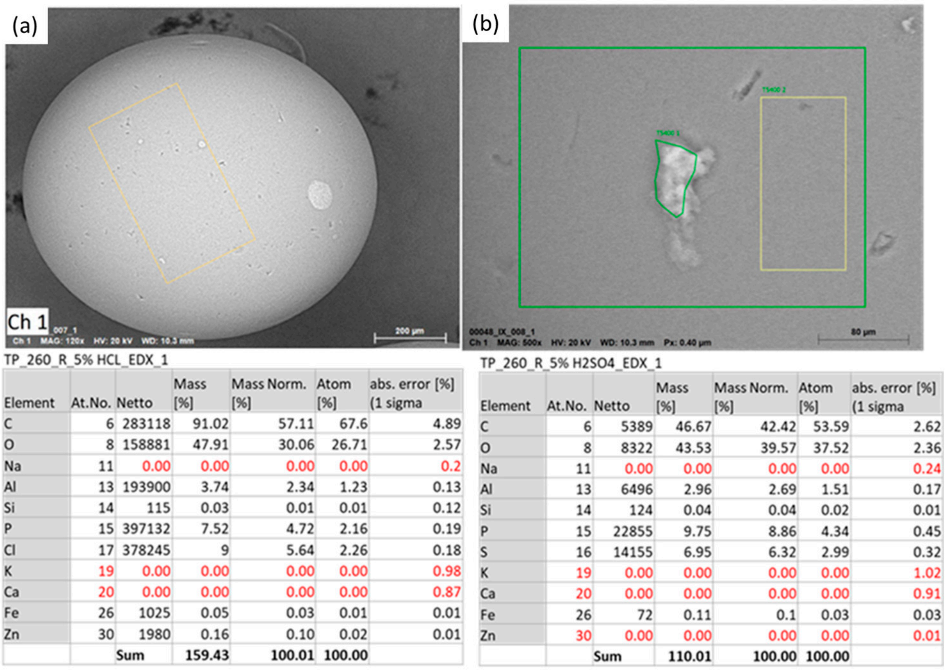

TP_260_R_5% HCL_EDX_1

Element	At.No.	Netto	Mass [%]	Mass Norm. [%]	Atom [%]	abs. error [%] (1 sigma
C	6	283118	91.02	57.11	67.6	4.89
O	8	158881	47.91	30.06	26.71	2.57
Na	11	0.00	0.00	0.00	0.00	0.2
Al	13	193900	3.74	2.34	1.23	0.13
Si	14	115	0.03	0.01	0.01	0.12
P	15	397132	7.52	4.72	2.16	0.19
Cl	17	378245	9	5.64	2.26	0.18
K	19	0.00	0.00	0.00	0.00	0.98
Ca	20	0.00	0.00	0.00	0.00	0.87
Fe	26	1025	0.05	0.03	0.01	0.01
Zn	30	1980	0.16	0.10	0.02	0.01
		Sum	**159.43**	**100.01**	**100.00**	

TP_260_R_5% H2SO4_EDX_1

Element	At.No.	Netto	Mass [%]	Mass Norm. [%]	Atom [%]	abs. error [%] (1 sigma
C	6	5389	46.67	42.42	53.59	2.62
O	8	8322	43.53	39.57	37.52	2.36
Na	11	0.00	0.00	0.00	0.00	0.24
Al	13	6496	2.96	2.69	1.51	0.17
Si	14	124	0.04	0.04	0.02	0.01
P	15	22855	9.75	8.86	4.34	0.45
S	16	14155	6.95	6.32	2.99	0.32
K	19	0.00	0.00	0.00	0.00	1.02
Ca	20	0.00	0.00	0.00	0.00	0.91
Fe	26	72	0.11	0.1	0.03	0.03
Zn	30	0.00	0.00	0.00	0.00	0.01
		Sum	**110.01**	**100.00**	**100.00**	

Figure 5. Elemental composition of used TP 260 resins (**a**) regenerated with 5% HCl acid (**b**) regenerated with 5% sulfuric acid.

These results indicate that traces of acid composition are visible on the resin surface even after washing the resins with distilled water. This might make the resin more acidic on the next loading cycle. Therefore, washing the resin with distilled water and subsequent conditioning is important to avoid problems in the long-term operation of the resin. Furthermore, it should be noted that both resins show small-scale patches (20–80 µm) on the resin surface, which might have been caused by the acids used in the de-loading process. More studies should be focused on the effect of acid concentration on metal recovery and resin life to enhance metal recovery while enhancing the lifetime of the resin as well.

2.7. Significant of Metal Recovery from Point Sources

Estimating elemental fluxes to the receiving rivers is essential to understanding the nature and the extent of the effect of mine discharge on the overall mass transport of the river system. The last detailed investigations of the three drainage tunnels date from the years 2000 and 2003 [54,55]. Even then, in comparison to measurements from the 1970s and 1980s, it was found that the content and loads in the tunnels were subject to a steady downward trend. To further investigate up-to-date trends of elemental fluxes, the estimated total fluxes (median value in g/min) in this study and the median elemental flux calculated by Degner [55] are compared in Table 4. It can be observed that the fluxes of earth alkalis (Mg and Ca), alkalis (Na and K), and Al have significantly reduced in VGS and RSS discharge. This can be attributed to the finite amount of elements in the pit that can be flushed out. However, HSU indicates an elevated flux of earth alkalis and alkalis in its discharge. Except for the total Fe flux at VGS, all three galleries show elevated fluxes of Fe and Mn at their discharge. Total Zn flux at the VGS and RSS indicates considerably lower values, while HSU indicates slightly higher values than the previous study. All three discharges indicate considerably lower sulfate load as well. Overall, all these weathering/or rock-dominated composition trends in the mine water will be merged later in the Elbe River system.

Table 4. Median Elemental Fluxes from Freiberg Mine Drainage Galleries to Receiving Rivers.

Load (Median) g/min	HSU		VGS		RSS	
	2003 [55]	2022	2003 [55]	2022	2003 [55]	2022
Na	51	96	140	67	1780	1021
K	11	16	19	10	250	141
Mg	65	80	178	76	970	697
Ca	180	261	410	240	3800	3097
Al	2.3	3	54	13	7.9	6
Fe	7.4	10	7	3	2.3	20
Mn	0.2	12	2	16	1.2	21
Si	NA	33	NA	18	NA	275
Zn	14	18	130	33	170	113
Cl	120	693	250	239	2180	2116
SO_4^{2-}	590	316	2200	851	11,700	7243

Al, Fe, Mn, and Zn are given as total loads; other elements in dissolved loads; NA—not available.

Generally, Ca, Mg, and Na mainly contributed to the solute fluxes among cations and SO_4^{2-} and Cl^- among anions. In particular, for trace elements, higher fluxes are relative to zinc. A calculation by Martin et al. [56] showed that about 37% of the total zinc load in the Elbe originates from the Freiberg mining area. Based on the comparison between this study and Degner [55], it can be assumed that the zinc load has considerably gone down throughout the last two decades. This study offers valuable insights, although a more complete understanding necessitates year-round data that incorporates extreme events, including snow melt and prolonged rains. Our simplified calculations indicate significant annual zinc discharges: a minimum of 26 tons from the VGS and HSU galleries to the Mulde river and 59 tons from the RSS gallery to the Triebisch River. Importantly, this research highlights the environmental impact of historic mining activities and proposes a solution. The showcased technique offers a two-fold benefit: treating mine water to remove harmful elements from recipient rivers and recovering them for potential reuse within a circular economy. Further research incorporating year-round data and extreme events could quantify the full extent of this issue and refine the proposed solution for even greater environmental impact.

3. Materials and Methods

3.1. Study Area

Freiberg is in the Saxon mining district and belongs to the Erzgebirge World Heritage area in central-eastern Germany (Figure 6). The annual mean rainfall in the study area is about 600 mm. The Freiberg polymetallic sulfide deposit was continuously exploited from 1168 to 1968. The deposit is mainly made up of two hydrothermal vein systems aged from the Late Variscian to the post-Variscian era [54]. Various researchers have also explored the potential environmental effects of the Freiberg mine [19,56–58].

The main underground working area extended into a network of different adits and reached a depth of 740 m below the surface level. At the beginning of the 19th century, the RSS gallery was constructed mainly to dewater the deeper water levels of the mine. Due to economic reasons, the mining activity was seized in 1968, and subsequently, part of the mine was flooded up to 225 m below the surface level, where the RSS is located [11]. The total amount of flooded mine working is around 2.6 million m^3, including mined-up ore bodies, waste dumps, and secondary filled materials [59].

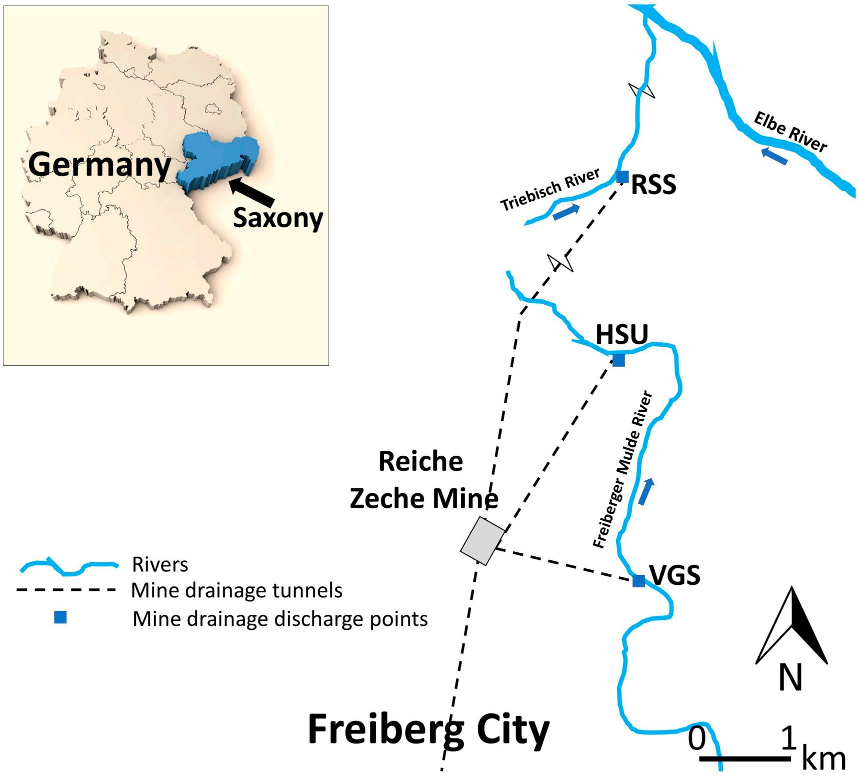

Figure 6. Location of the Reiche Zeche Mine and the important Mine drainage galleries "Verträgliche Gesellschaft Stolln" (VGS), "Rothschönberger Stolln" (RSS), "Hauptstolln Umbruch" (HSU).

The unflooded part of the mine is mainly composed of backfilled waste rocks, remnants of mined-out ore bodies, thin veins, and ore minerals within the host rocks. The mine water from some upper mining regions discharges via VGS and HSU into the Mulde river. The VGS water gallery forms the starting point of the Roter Graben, which diverts the mine water flowing out of several drainage tunnels (also HSU) into the Freiberger Mulde river [11]. Today, in addition to the infiltration water collected in the Freiberg mine galleries, cooling water from the Freiberg South industrial estate is discharged into the Roter Graben via the VGS. As water infiltrates through mine dumps and galleries, it becomes strongly enriched through dissolution. In the early 19th century, the HSU drainage gallery was built to improve drainage in the Freiberg mine because the water in old works repeatedly flowed into the deeper ground. After all, the wooden channels were leaking. HSU now mainly collects rainwater flowing through mountains/mine galleries via old adits and dewater into the Freiberger Mulde at the same level as VGS [11,54].

3.2. Mine Water Sampling and Preservation

This study collected water from the outflow of three adits (VGS, HSU, and RSS) and the recipient rivers from July 2021 to September 2021 and May 2022 to August 2022. First, the organoleptic assessment was made at the sampling site to inspect the smell, color, and turbidity. Then, electrical conductivity (EC25), pH, redox, and temperature were measured on-site with a daily calibrated multimeter (WTW Multi 3430, Wissenschaftlich-Technische Werkstätten GmbH, Weilheim, Germany). The flow rate at VGS and HSU discharge was determined with a "folding rule" by considering the outflow cross-section and the measured time of a "swimming body" over a distance of 2 m. The flow rates of the RSS discharge were taken from the automated probe installed at the site (which can be checked at www.umwelt.sachsen.de (accessed on 10 January 2023). In total, 61 water samples were collected in 8 sampling campaigns. We decided on two filtration steps (5 µm and 0.45 µm PSE membrane filters) for sample separation for compatibility purposes. Hereinafter, <0.45-µm fractions are termed "dissolved", and >0.45-µm fractions are termed "particulates" (colloidal and larger suspended particles). Daily water samples were collected and transported to the laboratory for storage at 4 °C. Subsequent chemical analysis was conducted using Microwave Plasma-Atomic Emission Spectroscopy (MP-AES, Agilent Technologies Deutschland GmbH, Waldbronn, Germany).

Apart from the water sampling explained above, in March 2023, a total volume of 1200 L of mine water from the VGS gallery was collected to conduct ion-exchange experiments to recover Zn as a secondary source of raw materials. The water was collected through a standing pump into 15 L smaller containers, which were then brought back to the laboratory to be stored in 300 L canisters for later experiments. All column experiments were started within one week of the water sampling.

3.3. Pretreatment of Mining-Influenced Water Before the Ion-Exchange Process

Considering the higher affinity of resin TP 260 towards aluminum (Al), a pretreatment strategy was developed to eliminate Al by precipitation. The primary objective of this strategy was the elimination of aluminum through precipitation, achieved by elevating the pH to 6.0. This pretreatment process preceded the ion-exchange experiment and was specifically designed to enhance the loading capacity for Zn on the resin. A preliminary small-scale experiment was conducted to establish the optimal conditions for precipitating all Al from the water samples. This experiment involved five water samples, each measuring one liter. The objective was to systematically assess the impact of different pH levels on aluminum precipitation. Various amounts of sodium hydroxide were systematically introduced into each water sample to attain targeted pH values from 4 to 8. The quantity of sodium hydroxide for each sample was determined using calculations using PHREEQC 3.0 (U.S. Geological Survey).

Subsequently, discrete samples were extracted from each treated sample after 24 h. The concentrations of zinc and aluminum in these samples were analyzed using MP-AES. This analytical technique was employed to identify the most efficient pH for aluminum precipitation, therefore establishing the optimal pretreatment step for the subsequent column experiment. Following the successful removal of aluminum, the treated water was filtrated using a 0.45 µm membrane filter to remove the precipitated Al (III) metals and any colloidal particles in the water.

3.4. Characterization of Ion-Exchange Materials

The TP 260 resin, also known as Lewatit TP 260 (Köln, Germany), is a macroporous IX resin incorporating an aminomethyl phosphonic acid chelating functional group. The resins were utilized without any prior conditioning steps. These resins were selected based on their predetermined affinity order for the elements available in the chosen water matrix. Table 5 provides an overview of the key properties of the resin. Lanxess Deutschland GmbH (Köln, NRW, Germany) supplied the resin samples. The application of scanning electron microscopy (SEM) in conjunction with energy-dispersive X-ray (EDX) analysis was utilized to examine the modifications in surface morphology and chemical composition of the resins during the IX process.

Table 5. Specifications and properties of the resins used in the study [52].

Property	**TP 260**
Structure	Macroporous weak acidic
Matrix	Crosslinked polystyrene
Functional group	Amino Methyl Phosphonic
Average particle size (mm)	0.85 ± 0.05
Uniformity coefficient	1.1
Bulk density (g/L)	709
Total exchange capacity (H form)	2.4 eq/L
pH range	2–10

3.5. Batch Adsorption Studies

The batch studies were carried out in two phases. In the first phase, the study was performed using synthetic water with zinc concentrations of 10 and 20 mg/L. The aqueous solutions were prepared by dissolving an appropriate quantity of zinc sulfate in the distilled water. The zinc sulfate was used in the crystallized form with the formula $ZnSO_4.7H_2O$. The batch experiments were carried out with 1000 mL of prepared solution and a fixed amount of TP 260 resin (from 0.1 mL to 2 mL). The solutions with resin were agitated for 24 h at 15 rpm until they reached the equilibrium state. The process was repeated for VGS mine waters with zinc concentrations of 10 and 20 mg/L. At the end, a sample from each canister was filtered, and the final concentration of the zinc in the solution was measured via MP-AES) to determine the adsorption capacity of the resin and the removal efficiency. All the experiments were carried out at room temperature. The zinc-adsorption capacity for different initial concentrations was calculated from

$$q_e = \frac{(C_0 - C_e)V}{m} \tag{1}$$

where q_e (mg/g) is the equilibrium adsorption capacity, C_0 is the initial concentration, and C_e is the equilibrium concentration of the intended ion in the solution. The volume of the solution represented by V (in liters) and m (in grams) is the mass of the resin. Ion-exchange isotherms can depict the relationship at constant temperature between the concentration of a dissolved substance (adsorbate) and the amount adsorbed per unit mass of the adsorbent material. Therefore, to gain a deeper understanding of the equilibrium data, the study utilized the Langmuir [60] and Freundlich [49] isotherm models, which are commonly found in scientific literature. These isotherm models can be used for characterizing heavy metal adsorption on adsorbates due to their simplicity and effectiveness in describing experimental data across a broad range of concentrations [46,47,61].

3.6. Column Experiments

In the ion exchange column setup, the process begins by introducing a solution containing metal ions into the resin bed. This continues until metal ions start to emerge from the opposite end of the column, indicating a breakthrough. Following conventional practice, the next step, often referred to as “regeneration”, entails extracting the adsorbed ions from the resin using a regenerant solution [38]. This process enables the resin to be reused in subsequent loading cycles. However, this study proposes substituting the term “regeneration” with “de-loading” to underscore the emphasis on recovering metal ions from the resins during this phase.

The column studies involved fixed-bed experiments using untreated mine waters (containing Fe and Al) as well as pretreated water (without Fe and Al). The primary objective was to evaluate the overall exchange capacity of the resin for Zn and compare the desorption behaviors of co-loaded ions by analyzing the loading and de-loading profiles. The experimental setup details are provided in Table 6. All four columns used in this study had dimensions of 1.5 cm in diameter and 12 cm in height, with a BV of 100 mL of wet-settled resin. The exact resin volume for the column (100 mL) was determined after immersing the fresh TP260 resin in distilled water for 24 h. Moreover, before the experiment, the column setup was tested with distilled water to remove trapped air. The columns were run with distilled water for 1 h to ensure the setup was completely packed with no possible cracks, channels, or unwanted voids. After loading, columns were flushed with 6 BVs of distilled water to remove excess ions from the system. The loading and de-loading processes were carried out at a flow rate of 10 BVs per hour. Regular samples were collected throughout the experiments to analyze a wide range of elements using MP-AES.

Table 6. Column experiment setup for the zinc recovery from mine waters of the VGS gallery.

	Resin	Column ID	Bed Volume (mL)	Flow Rate (BV/h)	De-Loading
Untreated VGS water	TP 260 (new)	V1	100	10	5%H_2SO_4
	TP 260 (new)	V2	100	10	5% HCl
Treated VGS water	TP 260 (new)	V3	100	10	5%H_2SO_4
	TP 260 (used)	V4	100	10	5%H_2SO_4

The first two columns, labeled V1 and V2, employed new TP 260 resin to extract zinc from untreated VGS water. V1 underwent de-loading with 5% H_2SO_4, while V2 utilized 5% HCl for de-loading. Similarly, two additional columns, denoted V3 and V4, were designated for use with pretreated VGS water, which had undergone aluminum removal via precipitation. In this setup, V3 utilized new TP 260 resin, while V4 employed previously used resin from V1. Both V3 and V4 columns underwent de-loading using 5% H_2SO_4.

3.7. Chemical Analyses

Sulfate levels were measured using the SulfaVer 4 method (Hach, Loveland, CO, USA), while chloride concentrations were determined using the LCK 311 method (Hach, Düsseldorf, Germany). Both analyses were conducted on water samples collected in 50 mL brown glass bottles without preservation, utilizing a Hach DR 3900 (spectrophotometer (Hach, Loveland, CO, USA). Element composition (Al, Ca, Fe, K, Mg, Mn, Na, P, S, Si, Zn), including major cations, was measured by MP-AES from the filtered and preserved water samples collected into 50 mL PE bottles. Minimum detection limits for cation measurements were 0.02 mg/L for Zn, Fe, and Al, and 0.01 mg/L for K, Ca, Si, As, Mn, and S. TIC/NPOC/TN were analyzed with the TOC-Analyzer Analytic Jena multi N/C 2100 S (Analytik Jena GmbH+Co. KG, Jena, Germany), using the water samples collected into 50 mL brown glass bottles without preservation. The accuracy and the precision of the analysis were verified against reference water and dilutions. Ion balance errors of the analyzed samples were verified using PHREEQC (3.0) geochemical code by incorporating the WATEQ4F database.

3.8. SEM-EDX Analyses

The surface morphology and chemical composition of the selected resins were analyzed using scanning electron microscopy with energy-dispersive X-ray spectroscopy (SEM-EDX). A HITHACHI-TM 4000 SEM device (Tokyo, Japan) was used, with an accelerating voltage of 15 to 20 kV for the characterization. Various magnifications were employed to observe the resin bead morphology. At the same time, EDX mapping was performed to determine the spatial distributions of targeted elements (Zn, Fe, and Al) at the same acceleration voltage. The resins were affixed to an aluminum stub holder with adhesive stickers. The initial state of the resins was assessed without any prior treatment. However, the resins deloaded with acids were washed with distilled water and dried before passed with the SEM-EDX.

4. Conclusions

This study demonstrates the feasibility of efficiently recovering metals from mining-influenced water using ion exchange. Given the selective range of ion-exchange resins toward different metals, pretreatment steps are often required to remove competitive ions before introducing the target metal ions into the ion-exchange circuit. In this study, the selective removal of competitive ions from the mining-influenced water effectively increased the zinc loading capacity of the resin from 0.2 eq/L to 1 eq/L. Under optimized conditions, the de-loading process produced an 18.5 g/L zinc concentrate with 100% recovery. Sulfuric acid demonstrated superior elution efficiency compared to hydrochloric acid. However, SEM-EDX analysis revealed residual acid on the resin surface even after washing with distilled water, which may affect the resin's performance in subsequent loading cycles.

Therefore, further research is needed to understand the long-term impacts of this residual acid on resin capacity. The study also estimated that three mine water galleries contribute approximately 85 tons of zinc annually to the Elbe River. Scaling up this technique to point sources of contamination, such as mine waste discharge points, could significantly reduce metal discharge into the environment. Additionally, the zinc concentrate produced could be used for research and development of new technologies or processes for zinc extraction, as well as exploring novel applications for zinc-based materials. It also holds potential for environmental remediation, such as soil stabilization, where zinc can help control pollution or promote plant growth. Therefore, these endeavors contribute to a circular economy and serve as a pivotal measure in environmental conservation.

Supplementary Materials: The following supporting information can be downloaded at: https://www.mdpi.com/article/10.3390/recycling9060105/s1, Figure S1: Linear presentation of Langmuir isotherm for Synthetic water and VGS water (10 and 20 mg/L zinc concentration); Figure S2: Zinc and aluminum removal from VGS water at different pH levels.

Author Contributions: Conceptualization, Writing—review and editing, Writing—original draft, Visualization, Validation, Software, Resources, Data curation, Formal analysis, Investigation, Methodology, J.A.; Writing—review and editing, Visualization, Validation, Software, Investigation, Formal analysis, Data curation, K.K.; Writing—review and editing, Supervision, Resources, Methodology, Formal analysis, M.G.; Writing—review and editing, Writing—original draft, Validation, Resources, Conceptualization, Investigation, Funding acquisition, Project administration, N.H.; Writing—review and editing, Validation, Resources, Conceptualization, Funding acquisition, Project administration, C.D. All authors have read and agreed to the published version of the manuscript.

Funding: This research project was conducted as part of the WasserWert project (support code 67EXI5036A), funded by the Federal Ministry for the Environment, Nature Conservation, Nuclear Safety, and Consumer Protection (BMUV) in Germany.

Data Availability Statement: The data presented in this study are available on request from the corresponding author.

Acknowledgments: The authors want to acknowledge Lanxess Deutschland GmbH for providing the resin samples. We also want to thank Erick Wolf, David Gärtner, and Godfrey Sechu for cooperating in sampling and laboratory experiments.

Conflicts of Interest: Author Marlies Grimmer was employed by the company Wismut GmbH. The remaining authors declare that the research was conducted in the absence of any commercial or financial relationship that could be construed as a potential conflict of interest.

References

1. Henckens, T. Scarce Mineral Resources: Extraction, Consumption and Limits of Sustainability. *Resour. Conserv. Recycl.* **2021**, *169*, 105511. [CrossRef]
2. Reynolds, S.; Anderson, L. Exploring Economic Adaptations: Qualitative Insights into the Metal Industry Amidst Shifting Towards Renewable Energy. *Preprint* **2023**. [CrossRef]
3. Aybarç, U.; Seydibeyoğlu, M.Ö. Recycling for a Sustainable World with Metal Matrix Composites. In *Recycling of Plastics, Metals, and Their Composites*; CRC Press: Boca Raton, FL, USA, 2021; ISBN 978-1-00-314876-0.
4. Leal, V.M.; Ribeiro, J.S.; Coelho, E.L.D.; Freitas, M.B.J.G. Recycling of Spent Lithium-Ion Batteries as a Sustainable Solution to Obtain Raw Materials for Different Applications. *J. Energy Chem.* **2023**, *79*, 118–134. [CrossRef]
5. Hudson-Edwards, K.A.; Jamieson, H.E.; Lottermoser, B.G. Mine Wastes: Past, Present, Future. *Elements* **2011**, *7*, 375–380. [CrossRef]
6. Kalisz, S.; Kibort, K.; Mioduska, J.; Lieder, M.; Małachowska, A. Waste Management in the Mining Industry of Metals Ores, Coal, Oil and Natural Gas—A Review. *J. Environ. Manag.* **2022**, *304*, 114239. [CrossRef]
7. Lottermoser, B.G. Recycling, Reuse and Rehabilitation of Mine Wastes. *Elements* **2011**, *7*, 405–410. [CrossRef]
8. Plumlee, G.S.; Morman, S.A. Mine Wastes and Human Health. *Elements* **2011**, *7*, 399–404. [CrossRef]
9. Mensah, M.K.; Drebenstedt, C.; Hoth, N.; Ola, I.M.; Okoroafor, P.U.; Wiafe, E.D. Artisanal Gold Mine Spoil Types within a Common Geological Area and Their Variations in Contaminant Loads and Human Health Risks. *Environ. Monit. Assess.* **2023**, *195*, 312. [CrossRef]
10. Moro, K.; Haubrich, F.; Martin, M.; Grimmer, M.; Hoth, N.; Schippers, A. Reductive Leaching Behaviour of Manganese and Cobalt Phases in Laterite and Manganese Ores. *Hydrometallurgy* **2023**, *220*, 106101. [CrossRef]

11. Wolkersdorfer, C. *Water Management at Abandoned Flooded Underground Mines: Fundamentals, Tracer Tests, Modelling, Water Treatment*; Springer Science & Business Media: Berlin/Heidelberg, Germany, 2008; ISBN 978-3-540-77331-3.
12. Agboola, O.; Babatunde, D.E.; Isaac Fayomi, O.S.; Sadiku, E.R.; Popoola, P.; Moropeng, L.; Yahaya, A.; Mamudu, O.A. A Review on the Impact of Mining Operation: Monitoring, Assessment and Management. *Results Eng.* **2020**, *8*, 100181. [CrossRef]
13. Lu, P.; Zhou, L.; Cheng, S.; Zhu, X.; Yuan, T.; Chen, D.; Feng, Q. Main Challenges of Closed/Abandoned Coal Mine Resource Utilization in China. *Energy Sources Part Recovery Util. Environ. Eff.* **2020**, *42*, 2822–2830. [CrossRef]
14. Wolkersdorfer, C.; Mugova, E. Effects of Mining on Surface Water. In *Encyclopedia of Inland Waters*; Elsevier: Amsterdam, The Netherlands, 2022; pp. 170–188. ISBN 978-0-12-822041-2.
15. Bouzek, J.; Koutecký, D.; Simon, K. Tin and Prehistoric Mining in the Erzgebirge (Ore Mountains): Some New Evidence. *Oxf. J. Archaeol.* **1989**, *8*, 203–212. [CrossRef]
16. Kvet, R. Mineral Mining on the Bohemian Side of the Krušné Hory Mountains/Erzgebirge up to the Time of Agricola. *GeoJournal* **1994**, *32*, 101–102. [CrossRef]
17. Jelen, J. Mining Heritage and Mining Landscape Krušnohoří/Erzgebirge as a Part of the UNESCO Heritage. *Land* **2022**, *11*, 955. [CrossRef]
18. Haubrich, F.; Tichomirowa, M. Sulfur and Oxygen Isotope Geochemistry of Acid Mine Drainage—The Polymetallic Sulfide Deposit “Himmelfahrt Fundgrube” in Freiberg (Germany). *Isot. Environ. Health Stud.* **2002**, *38*, 121–138. [CrossRef]
19. Zhiteneva, V.; Brune, J.; Mischo, H.; Weyer, J.; Simon, A. Water Quality of Reiche Zeche Teaching Mine, Freiberg, Saxony, Germany. In Proceedings of the SME Annual Meeting, Phoenix, AZ, USA, 21–24 February 2016.
20. Junghans, M.; Tichomirowa, M. Using Sulfur and Oxygen Isotope Data for Sulfide Oxidation Assessment in the Freiberg Polymetallic Sulfide Mine. *Appl. Geochem.* **2009**, *24*, 2034–2050. [CrossRef]
21. Tichomirowa, M.; Heidel, C.; Junghans, M.; Haubrich, F.; Matschullat, J. Sulfate and Strontium Water Source Identification by O, S and Sr Isotopes and Their Temporal Changes (1997–2008) in the Region of Freiberg, Central-Eastern Germany. *Chem. Geol.* **2010**, *276*, 104–118. [CrossRef]
22. Stockmann, M.; Hirsh, D.; Lippmann-Pipke, J.; Kupsch, H. Geochemical Study of Different-Aged Mining Dump Materials in the Freiberg Mining District, Germany. *Environ. Earth Sci.* **2013**, *68*, 1153–1168. [CrossRef]
23. Nobahar, A.; Melka, A.B.; Marín-Beltrán, I.; Neves, L.; Costa, M.C.; Carlier, J.D. Zinc Recovery from an Extreme Copper-Free Acid Mine Drainage: Studying the Prior Separation of Ferric Iron by Solvent Extraction Using AliCy and/or Alkalinization. *J. Sustain. Metall.* **2022**, *8*, 1509–1531. [CrossRef]
24. Reichl, C.; Schatz, M. *World Mining Data 2020*; Federal Ministry of Agriculture Regions and Tourism: Vienna, Austria, 2020; Volume 35.
25. Fu, F.; Wang, Q. Removal of heavy metal ions from wastewaters: A review. *J. Environ. Manag.* **2011**, *92*, 407–418. [CrossRef]
26. Vahidi, E.; Rashchi, F.; Moradkhani, D. Recovery of Zinc from an Industrial Zinc Leach Residue by Solvent Extraction Using D2EHPA. *Miner. Eng.* **2009**, *22*, 204–206. [CrossRef]
27. Fernando, W.A.M.; Ilankoon, I.M.S.K.; Syed, T.H.; Yellishetty, M. Challenges and Opportunities in the Removal of Sulphate Ions in Contaminated Mine Water: A Review. *Miner. Eng.* **2018**, *117*, 74–90. [CrossRef]
28. Johnson, D.B. Biomining-Biotechnologies for Extracting and Recovering Metals from Ores and Waste Materials. *Curr. Opin. Biotechnol.* **2014**, *30*, 24–31. [CrossRef]
29. Doyle, S.; Figueroa, L. Removal of Molybdenum from Mining-Impacted Water by Sorption onto Manganese-Rich Sludge. *Mine Water Environ.* **2022**, *41*, 721–730. [CrossRef]
30. Ryu, S.; Naidu, G.; Hasan Johir, M.A.; Choi, Y.; Jeong, S.; Vigneswaran, S. Acid Mine Drainage Treatment by Integrated Submerged Membrane Distillation–Sorption System. *Chemosphere* **2019**, *218*, 955–965. [CrossRef]
31. Gan, Y.; Ding, C.; Xu, B.; Liu, Z.; Zhang, S.; Cui, Y.; Wu, B.; Huang, W.; Song, X. Antimony (Sb) Pollution Control by Coagulation and Membrane Filtration in Water/Wastewater Treatment: A Comprehensive Review. *J. Hazard. Mater.* **2023**, *442*, 130072. [CrossRef] [PubMed]
32. Timofeev, K.L.; Kurdiumov, V.; Maltsev, G. Sorption and Membrane Technologies for Mine Water Purification. *Mater. Sci. Forum* **2019**, *946*, 621–627. [CrossRef]
33. Abeywickrama, J.; Grimmer, M.; Hoth, N. Recovery of Strategically Important Heavy Metals from Mining Influenced Water. In *Hybridized Technologies for the Treatment of Mining Effluents*; John Wiley & Sons, Ltd.: Hoboken, NJ, USA, 2023; pp. 41–78. ISBN 978-1-119-89692-0.
34. van Deventer, J. Selected Ion Exchange Applications in the Hydrometallurgical Industry. *Solvent Extr. Ion Exch.* **2011**, *29*, 695–718. [CrossRef]
35. Botelho, A.B.; Espinosa, D.C.R.; Dreisinger, D.; Tenório, J.A.S. Effect of pH to Recover Cu(II), Ni(II) AND Co(II) from Nickel Laterite Leach Using Chelating Resins. *Tecnol. Metal. Mater. Min.* **2019**, *16*, 135–140. [CrossRef]
36. Sole, K.C. Present and Future Applications of Ion Exchange in Hydrometallurgy: An Overview. In Proceedings of the IEX 2016, The International Ion Exchange Conference, Cambridge, UK, 6–8 July 2016; pp. 2–33.
37. Sole, K.C. The Evolution of Cobalt–Nickel Separation and Purification Technologies: Fifty Years of Solvent Extraction and Ion Exchange. In *Extraction 2018: Proceedings of the First Global Conference on Extractive Metallurgy, Ottawa, ON, Canada, 26–29 August 2018*; Davis, B.R., Moats, M.S., Wang, S., Gregurek, D., Kapusta, J., Battle, T.P., Schlesinger, M.E., Alvear Flores, G.R., Jak, E., Goodall, G., et al., Eds.; Springer International Publishing: Cham, Switzerland, 2018; pp. 1167–1191.

38. Harland, C.E. *Ion Exchange*; Royal Society of Chemistry: London, UK, 1994; ISBN 978-0-85186-484-6.
39. Littlejohn, P.; Vaughan, J. Recovery of Nickel and Cobalt from Laterite Leach Tailings through Resin-in-Pulp Scavenging and Selective Ammoniacal Elution. *Miner. Eng.* **2013**, *54*, 14–20. [CrossRef]
40. Pedregal Montes, A.I.; Abeywickrama, J.; Hoth, N.; Grimmer, M.; Drebenstedt, C. Modeling of Ion Exchange Processes to Optimize Metal Removal from Complex Mine Water Matrices. *Water* **2021**, *13*, 3109. [CrossRef]
41. Abeywickrama, J.; Hoth, N.; Ussath, M.; Drebenstedt, C. Selective Extraction of Cobalt and Copper from Chilean Mine Water by Ion Exchange Resin. *Gorn. Nauk. Tekhnol. Min. Sci. Technol. Russ.* **2020**, *5*, 25–29. [CrossRef]
42. Choi, J.-W.; Song, M.-H.; Bediako, J.K.; Yun, Y.-S. Sequential Recovery of Gold and Copper from Bioleached Wastewater Using Ion Exchange Resins. *Environ. Pollut.* **2020**, *266*, 115167. [CrossRef]
43. Aşçı, Y.; Kaya, Ş. Removal of Cobalt Ions from Water by Ion-Exchange Method. *Desalin. Water Treat.* **2014**, *52*, 267–273. [CrossRef]
44. Strauss, M.L.; Diaz, L.A.; McNally, J.; Klaehn, J.; Lister, T.E. Separation of Cobalt, Nickel, and Manganese in Leach Solutions of Waste Lithium-Ion Batteries Using Dowex M4195 Ion Exchange Resin. *Hydrometallurgy* **2021**, *206*, 105757. [CrossRef]
45. Abeywickrama, J.; Hoth, N.; Grimmer, M.; Haubrich, F.; Drebenstedt, C. Optimizing Metal Recovery from Slag Leaching Solutions: Advanced Ion Exchange Techniques for Sustainable Resource Extraction. *J. Water Process Eng.* **2023**, *56*, 104482. [CrossRef]
46. Bezzina, J.P.; Robshaw, T.; Dawson, R.; Ogden, M.D. Single Metal Isotherm Study of the Ion Exchange Removal of Cu(II), Fe(II), Pb(II) and Zn(II) from Synthetic Acetic Acid Leachate. *Chem. Eng. J.* **2020**, *394*, 124862. [CrossRef]
47. Felipe, E.C.B.; Batista, K.A.; Ladeira, A.C.Q. Recovery of Rare Earth Elements from Acid Mine Drainage by Ion Exchange. *Environ. Technol.* **2021**, *42*, 2721–2732. [CrossRef]
48. Hermassi, M.; Granados, M.; Valderrama, C.; Skoglund, N.; Ayora, C.; Cortina, J.L. Impact of Functional Group Types in Ion Exchange Resins on Rare Earth Element Recovery from Treated Acid Mine Waters. *J. Clean. Prod.* **2022**, *379*, 134742. [CrossRef]
49. Debord, J.; Chu, K.H.; Harel, M.; Salvestrini, S.; Bollinger, J.-C. Yesterday, Today, and Tomorrow. Evolution of a Sleeping Beauty: The Freundlich Isotherm. *Langmuir* **2023**, *39*, 3062–3071. [CrossRef]
50. Bao, S.; Hawker, W.; Vaughan, J. Scandium Loading on Chelating and Solvent Impregnated Resin from Sulfate Solution. *Solvent Solvent Extr. Ion Exch.* **2018**, *36*, 100–113. [CrossRef]
51. Liu, Y. Fluoride Removal from Zinc Sulfate Solution. Master's Thesis, University of British Columbia, Vancouver, BC, Canada, 2017.
52. Lanxess LEWATIT-MonoPlus-TP-260 2019. Available online: https://lanxess.com/en-us/products-and-brands/products/l/lewatit--monoplus-tp-260 (accessed on 10 May 2024).
53. Taute, J.; Sole, K.; Hardwick, E. Zinc Removal from a Base-Metal Solution by Ion Exchange: Process Design to Full-Scale Implementation. In Proceedings of the Southern African Institute of Mining and Metallurgy Base Metals Conference, Mpumalanga, South Africa, 2–4 September 2013.
54. Baacke, D. Geochemisches Verhalten umweltrelevanter Elemente in stillgelegten Polysulfiderzgruben am Beispiel der Grube "Himmelfahrt" in Freiberg Sachsen. Ph.D. Dissertation, TUBA Freiberg, Freiberg, Germany, 2000. Available online: http://webdoc.sub.gwdg.de/ebook/diss/2003/tu-freiberg/archiv/html/Geowissenschaften_BaackeDelf966689.html (accessed on 4 December 2022).
55. Degner, T. Prognose von Geochemischen Auswirkungen der Nachnutzung Stillgelegter Bergbau-Stollen-Systeme am Beispiel des Freiberger Grubenreviers. Ph.D. Thesis, Freiberg University of Mining and Technology, Freiberg, Germany, 2003.
56. Martin, M.; Beuge, P.; Kluge, A.; Hoppe, T. *Grubenwässer des Erzgebirges—Quelle von Schwermetallen in Der Elbe*; Spektrum der Wissenschaft: Heidelberg, Germany, 1994; pp. 102–107.
57. Baumann, L.; Kuschka, E.; Seifert, T. *Lagerstätten Des Erzgebirges*; Enke im Thieme Verlag: Stuttgart, Germany, 2000; p. 300.
58. Knittel, U.; Klemm, W.; Greif, A. Heavy Metal Pollution Downstream of Old Mining Camps as a Result of Flood Events: An Example from the Mulde River System, Eastern Part of Germany. *TAO Terr. Atmos. Ocean. Sci.* **2005**, *16*, 919–931. [CrossRef]
59. Kolitsch, S.; Junghans, M.; Klemm, W.; Tichomirova, M. Der Flutungsraum Des Grubenfeldes Freiberg—Hydrochemie, Isotopenchemie Und Hydraulik. *Wiss. Mitt.* **2001**, *18*, 14–26.
60. Langmuir, I. The Adsorption of Gases on Plane Surfaces of Glass, Mica and Platinum. *J. Am. Chem. Soc.* **1918**, *40*, 1361–1403. [CrossRef]
61. Wang, J.; Guo, X. Adsorption Isotherm Models: Classification, Physical Meaning, Application and Solving Method. *Chemosphere* **2020**, *258*, 127279. [CrossRef]